

KINETIC MODEL FOR IDENTIFYING THE RATE CONTROLLING STEP OF THE ALUMINUM LEACHING FROM PEAT CLAY

Agus Mirwan, Susianto, Ali Altway, Renanto Handogo*

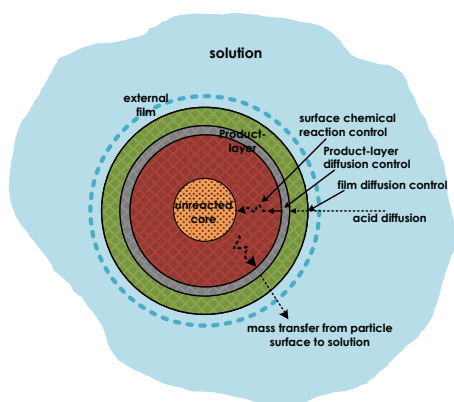
Department of Chemical Engineering, Faculty of Industrial Technology, Institut Teknologi Sepuluh Nopember, Surabaya 60111, Indonesia

Article history

Received
19 April 2017
Received in revised form
2 September 2017
Accepted
10 January 2017

*Corresponding author
renanto@chem-eng.its.ac.id

Graphical abstract



Abstract

The aluminum (Al) leaching kinetics from peat clay was investigated using various acid concentrations 1 M to 6 M, particle sizes +70-120 mesh to +200-325 mesh and temperatures 30 °C to 90 °C. They all have significant effects on aluminum leaching process. The Al leaching recovery was best found to be 91.3 % at 4 M hydrochloric acid (HCl), using a particle size of +200-325 mesh with solid/liquid of 0.02 g·mL⁻¹. Leaching kinetic study was applied to the two rate equations proposed that is acid diffusion via product layer and surface chemical reaction using the shrinking core (SC) model to analyze the leaching data. The product layer diffusion is controlling Al leaching process for one-stage model, while for two-stage model, it was controlled by surface chemical reaction. The activation energy in the two rate controlling step was 82.79 kJ mol⁻¹ and 27.08 kJ mol⁻¹, respectively.

Keywords: Aluminum, kinetics, leaching, one-stage, peat clay, two-stage

© 2018 Penerbit UTM Press. All rights reserved

1.0 INTRODUCTION

Peatlands are the environmental transition between terrestrial and aquatic ecosystems [1] that indicated by the existence of naturally accumulated peat sheets. Peat clay is clay soil which located at a depth of about 1.5 to 3.0 meters from the peat soil. In Indonesia, especially in South Kalimantan, peatlands are very spacious and they have not been utilized optimally. Indirectly, their existence shows that there are a lot of peat clay. The main mineral of peat clays generally has a major chemical composition in the form of aluminum oxide (Al₂O₃) in which it has potential as a coagulant, adsorbents and catalysts for use in wastewater treatment [2]. Aluminium (Al) is the most abundant metal and the third largest element contained in the Earth's crust, which contained in the mineral, rock, and

clay, like a peat clay containing Al salts. According to chemical analyses data, silica oxide (SiO₂) and Al₂O₃ are major elements.

The methods for leaching of Al can generally be encapsulated into alkaline and acid methods. Leaching process of Al requires prior activation process because of its inactive and stable structure. A very common method to activate the clay by thermal treatment. This process is expected to increase the clay reactivity that influences the dehydration transformation of kaolinite to amorphous meta kaolinite (Al₂SiO₇), which is more reactive and easy to extracted with acids or alkaline [3]. The alkaline method is not appropriate for Al extraction, however, the acid method has the benefit for short process, low energy consumption, less residue, and easy and complete separation of Al. Various mineral acid for leaching Al have been investigated and shown in Table 1.

Table 1 Literature reported studies on Al leaching

Leaching agent	Condition	Material	Percent recovery	Ref
H ₂ SO ₄	700 °C and 120 min, 40% wt H ₂ SO ₄ , 65 mesh, 0.88 g/ml 120 min, boiling condition	Clay from Az-Zabirah, Saudi Arabia	88.5	Al-Zahrani and Abdul-Majid [6]
HCl	560–750 °C and 30–45 min, 28% wt HCl, 15, 45 min, 100 °C ± 5	Kaolin from Duwaikhla Mine, Iraq	93	Al-Ajeel and Al-Sindy [7]
HCl	600 °C and 120 min, 3 M HCl, -100 mesh, 0.1 g/ml, 120 min, boiling condition	Clay from Riyadh, Saudi Arabia	62.9	Al-Zahrani and Abdul-Majid [8]
NaOH	6.25 M NaOH, 0.067 g/ml, 800–900 rpm, 180 min, 95 °C	Iron ore from Joda mine, India	80	Sakar [9]
HNO ₃	650 °C and 80 min, 6 M HNO ₃ , 0.045 mm, 0.02 g/ml, 540 rpm, 20–150 min, 100 °C	Clay from Ukpor mine, Nigeria	81.7	Ajemba and Onukwuli [10]
HCl	750 °C and 240 min, 4.8 M HCl, 0.045 mm, 0.02 g/ml, 540 rpm, 200 min, 90 °C	Clay from Ukpor mine, Nigeria	90	Ajemba and Onukwuli [16]
H ₂ SO ₄	750 °C and 30 min, 3 M H ₂ SO ₄ , -200 mesh, 0.8 g/ml, 120 min, 100 °C	Lampang clays from Thailand	95.1	Numluk and Chaisena [11]
HCl	650 °C and 160 min, 8 N HCl, -200 mesh, 0.1 g/ml, 720 min, 90 °C	Kaolinitic clay from Sinai at El-Tih, Egypt	77.3	Ibrahim, et al. [12]
H ₂ SO ₄	700 °C and 120 min, 1.5 M H ₂ SO ₄ , 3–5.4 µm, 180 min, 95 °C	Kaolin from the Capim region, Brazil	99.6	Lima, et al. [13]
NH ₄ Cl/NH ₄ NO ₃	70 °C and 480 min, 0.2 M NH ₄ , 1:1 NHCl/NH ₄ NO ₃ , 360 min, 25 °C	Rare earth ore from Dingnan, Jiangxi Province, China	89.1	He, et al. [14]

Among these acids, hydrochloric acid has several advantages, especially for the treatment of pure kaolinitic clay. At ambient temperature, Al₂O₃ cannot react with acid. However, only aluminium hydroxide (Al(OH)₃) shaped amorphous solid can be leached under acidic conditions. Hence, the major reaction of aluminum oxide with acid is the following:



The leaching of Al with hydrochloric acid is represented as a non-catalytic leaching reactions with aluminum grains assumed to be dispersed evenly throughout the particle such that the entire solid may be considered to act as a homogeneous reactant. The rate of conversion is dependent upon the current state of the leaching and the concentration of the acid in the fluid surrounding the particle [4]. This modelling is usually done using the shrinking core (SC) model. SC model assumes that the solute is located inside the core solid particle that shrinks as the extracted solute, and assumes first-order reaction and unchanged structure of the particles [5].

Each particle is considered to be a sphere of initially unreacted material. Diffusion and chemical reaction processes take place on the surface of the sphere and then progresses inwards, such that the core of unreacted material shrinks and leaves behind a layer of inert, permeable, solid product at the irreversible desorption condition. Many studies using SC model have been done on leaching kinetics from clay. Most of them focus on thermal treatment, solid-liquid ratio, acid concentration, particle size, temperature, and whole reaction time, which is influencing leaching kinetics behavior (Table 2).

In fact, hydrochloric acid leaching is affected by a variety of parameters (acid contraction, particle size, and reaction temperature as a function of whole leaching time). However, The leaching kinetics of aluminum from peat clay at difference of leaching time (one-stage and two-stage) has never existed. In the present study, The effects of four different acid concentration, three different particle sizes, and four different of reaction temperature as a function of different leaching time were evaluated. Leaching kinetics of Al were examined according to non-catalytic fluid–solid reaction using SC model for determining the rate controlling steps at one-stage and two-stage.

2.0 METHODOLOGY

2.1 Materials

Peat clay was collected from Peat Village, Subdistrict of Peat, District of Banjar, South Kalimantan, Indonesia with longitude coordinates of location between 3°23'55.3"S and 114°42'14.6"E and in the depths about 3.0 meters from the surface of the earth. Peat clay was washed and dried under direct sunlight 48 hours and then it was crushed and screened with size fraction of +70-325 mesh (0.044-0.210 mm) based on a standard sieve of the American Society for Testing and Materials (ASTM) and calcined at 700 °C for 2 hours for thermal treatment. HCl was gained from Sigma-Aldrich with a purity of 37%. Required concentrations of HCl were arranged along with dilution of deionized water.

Table 2 Kinetic models for leaching process of Al

Time, t/min	Temperature, T/°C	Rate-controlling step	Activation energy, E _a /kJ mol ⁻¹	Leaching kinetic model	Ref
300	45–96	Chemical reaction	79	$\frac{t}{\tau} = 1 - (1 - x)^{1/3}; \tau = \frac{\rho_B R_0}{b k_s C_A}$ $k_s = \exp(8.55 - 9500 / T) m / s$	Altiokka and Hoşgün [15]
20–150	100	Product-layer diffusion	30.5	$1 + 2(1 - x) - 3(1 - x)^{2/3}$ $= 0.96 \times 10^2 C_{[HNO_3]}^{0.52} (d_p)^{-1.73} (s / l)^{-0.66}$ $(w)^{0.68} e^{-30.521/RT}$	Ajemba and Onukwuli [10]
200	90	Product-layer diffusion	39	$1 + 2(1 - x) - 3(1 - x)^{2/3}$ $= 1.40 \times 10^3 C_{[HCl]}^{0.37} (d_p)^{-0.89} (s / l)^{-0.63}$ $(w)^{0.42} \exp(-4677 / T)t$	Ajemba and Onukwuli [16]
180	95	Chemical reaction	97.7	-	Lima, et al. [13]
600	25	Product-layer diffusion	1.5	$1 + \frac{2}{3} a - (1 - a)^{2/3} = 0.0062 C_0^{1.48} t$	He, et al. [14]

2.2 Leaching Process

The leaching process had been done in an atmospheric Iwaki Pyrex reactor which it had two necks for a thermometer and for the inlet and/or outlet of the sample at regular intervals. The mixing reaction process is using a magnetic stirrer at 300 r min⁻¹ and heated indirectly via a water bath. Al leaching from the calcined peat clay was reacted in the reactor using several of HCl concentration, particle sizes, and reaction temperatures as the function of time. 5 g of calcined peat clay was added to 250 ml agitated HCl solution (solid/liquid ratio is 0.02 g ml⁻¹) at a particular temperature. The effect of acid concentration (1, 2, 4, and 6 M), particle size (+70-120, +120-200, and +200-325 mesh), and reaction temperature (30, 50, 70, and 90 °C) on Al leaching was studied and performed at 60 min. At selected time interval, all samples were collected using a syringe and filtered for analysis determine aluminum content in solution using inductively coupled plasmacluster optical emission spectrometer (ICP-OES) (9060-D Teledyne Leeman Labs. USA). Each analysis was repeated three times and deputized with average values. The Al leaching ratio (x) can be calculated as:

$$x = X/X_0 \quad (2)$$

where X₀ denotes total Al obtained through acid leaching process and X is the amount of Al obtained at different conditions (mg/g).

2.3 Shrinking Core (SC) Model

The SC model for unchanging structure and size of spherical particles [17] describes kinetic characteristics of reaction mechanisms throughout

the noncatalytic heterogeneous solid-liquid reaction. There is three mechanisms process system in the surface reaction of the solid-liquid system which comprises of the following: film diffusion, product-layer diffusion, and surface chemical reaction [18,19]. In this study, however, only two reaction mechanisms would be used at previously established SC model [20–23]. The kinetics equation for leaching proses controlled by a surface chemical reaction is as follows:

$$\frac{t}{\tau_c} = 1 - (1 - x)^{1/3} \quad (3)$$

If the product-layer diffusion is controlling the leaching process, the kinetics equation as follows:

$$\frac{t}{\tau_c} = 1 - 3(1 - x)^{2/3} + 2(1 - x) \quad (4)$$

With the complete leaching time by surface chemical reaction control $\tau_c = \rho_B R / b M_w k_c C_A$ and the complete leaching time by-product layer diffusion control $\tau_i = \rho_B R^2 / 6 b M_w D_e C_A$, where x denotes the aluminum leaching recovery fraction; t is the reaction time; ρ_B is the solid density; R is the radius of initial particle; b is the stoichiometric coefficient; M_w is the molecular weight (g/mol); k_c is the factor of mass transfer; C_A is hydrochloric acid concentration; and D_e is the coefficient of product layer diffusion.

Equation (3) and (4) can be applied to one-stage leaching. If the model does not follow the experimental data; then a two-stage leaching can be used. However, for two-stage, the boundary condition is different with the condition of one-stage. In this case,

the modified equations can be formulated as follows [24]:

$$\frac{t - t_1}{\tau_C} = 1 - \left(\frac{1-x}{1-x_1} \right)^{1/3} \quad (5)$$

$$\frac{t - t_1}{\tau_C} = 1 - 3 \left(\frac{1-x}{1-x_1} \right)^{2/3} + 2 \left(1 - (1-x_1)^{1/3} \right) (x-x_1) \quad (6)$$

with complete leaching time by surface chemical reaction control $\tau_C = \rho_B R (1-x_1) / b M_W k_C C_A$ and complete leaching time by-product layer diffusion control at a long period of time $\tau_i = \rho_B R^2 (1-x_1)^{2/3} / 6 b M_W D_e C_A$, where t_1 and x_1 values are not zero and its value from experimental data should be regarded as an initial condition.

3.0 RESULTS AND DISCUSSION

3.1 Characterization of Peat Clay Particle

Characterization of peat clay was analyzed with XRD (Philips X-pert powder model, Netherlands) and identified by comparing 'd' values using powder diffraction data base file-2 (PDF-2) 1996. The possible minerals with their 'd' values present the major mineral phases i.e. kaolinite ($\text{Al}_2\text{Si}_2\text{O}_5(\text{OH})_4$), quartz (SiO_2), hematite Fe_2O_3 , and corundum (Al_2O_3) (Figure 1).

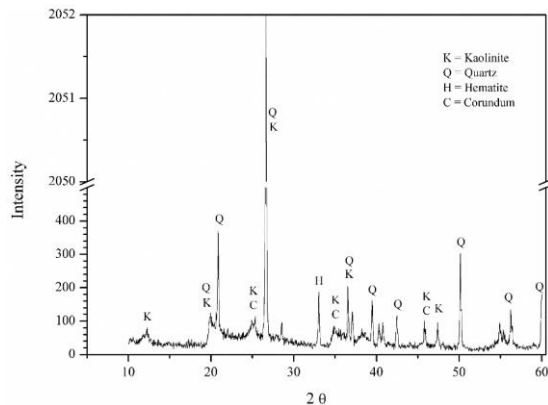


Figure 1 XRD pattern of peat clay from Peat Village, Subdistrict of Peat, District of Banjar, South Kalimantan, Indonesia

FTIR studies help in the identification of various forms of the minerals present in the peat clay. The coupled vibrations are appreciable due to the availability of various constituents. Identification of variations mineral form of each functional group which brought distinctive properties of the compounds in the peat clay using FTIR (Shimadzu, Japan). Observed bands (in the range, 4000–500 cm^{-1}) have been tentatively assigned. The results are shown in Figure 2 and Table 3.

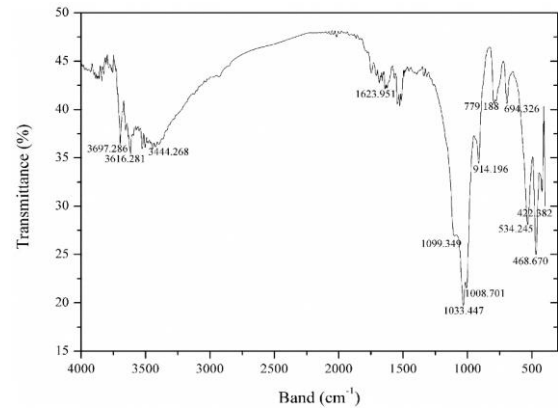


Figure 2 FTIR spectrum of peat clay from Peat Village, Subdistrict of Peat, District of Banjar, South Kalimantan, Indonesia

Table 3 Infrared spectroscopy (IR) band of peat clay from Peat Village, Subdistrict of Peat, District of Banjar, South Kalimantan, Indonesia

Infrared Band (cm ⁻¹)	Transmittance (%)	Assignment
3697.29	36.350	Al–O–H str (kaolinite, illite)
3616.28	35.428	Al–O–H (kaolinite, illite, calcite)
3444.63	35.979	H–O–H str (kaolinite, illite)
1623.95	42.233	H–O–H str (illite, calcite)
1099.35	26.901	Si–O str (kaolinite, quartz)
1033.77	19.707	Si–O–Si, Si–O str. (kaolinite, illite)
1008.7	21.507	Si–O str (kaolinite, quartz)
914.2	34.436	Al–O–H str (kaolinite, illite, hematite)
779.19	40.861	Si–O–Al str (kaolinite, illite)
694.33	40.595	Si–O str., Si–O–Al str (quartz, kaolinite)
534.25	28.083	Si–O str., Si–O–Al str (kaolinite)
468.67	25.018	Si–O str., Si–O–Fe str. (quartz, kaolinite)
422.38	31.474	Si–O str (quartz)

Flake structure of peat clay was analyzed by SEM-EDX (SEM EVO MA 10, Germany) that showed the presence of the same dominant elements, namely Al, Si, Fe (color difference) with a composition of 31.21%wt, 50.18%wt, 18.61%wt respectively (Figure 3).

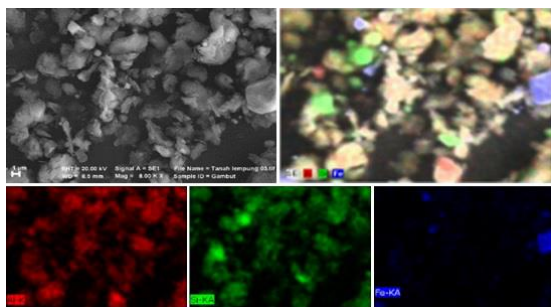


Figure 3 Morphology SEM of peat clay from Peat Village, Subdistrict of Peat, District of Banjar, South Kalimantan, Indonesia

XRF characterization was performed to know the chemical compositions of the minerals that are present in the peat clay. The chemical composition of peat clay based on XRF (PANalytical miniPAL4, Netherlands) analysis is listed in Table 4. The aluminum oxide, silica oxide, and iron oxide are present in major quantities while other minerals are present in trace amounts.

Table 4 Chemical composition of peat clay from Peat Village, Subdistrict of Peat, District of Banjar, South Kalimantan, Indonesia

Compound	Mass composition %
SiO ₂	38.80
Al ₂ O ₃	11.00
Fe ₂ O ₃	27.00
K ₂ O	1.16
MnO	0.10
CaO	0.83
TiO ₂	2.57
V ₂ O ₅	0.11
Cr ₂ O ₃	0.20
ZnO	0.06
NiO	0.93
CuO	0.16
MoO ₃	6.50
Re ₂ O ₇	0.10
LOI	10.48

3.2 Effect of Acid Concentration

Figure 4 indicates that Al leaching ratio increases with increasing acid concentration from 1 M to 6 M. When at 6 M of HCl, however, it decreased slightly in all leaching time. This result could possibly be caused by the settling of metal-chloride [25]. The viewpoint of leaching kinetics that increasing Al leaching ratio along with increasing concentrations of HCl, but, the decrease in the solubility of aluminum chloride (AlCl₃). In accordance with Cui, *et al.* [25] when AlCl₃ is saturated dissolution and precipitation of aluminum oxide (Al₂O₃) have been occurred a dynamic stability, wherein Al₂O₃ dissolution percentage was reached a stable condition. This might describe the aluminum leaching ratio behavior in 6 M of HCl solution. The HCl

concentration of 4 M was therefore chosen for subsequent experiments.

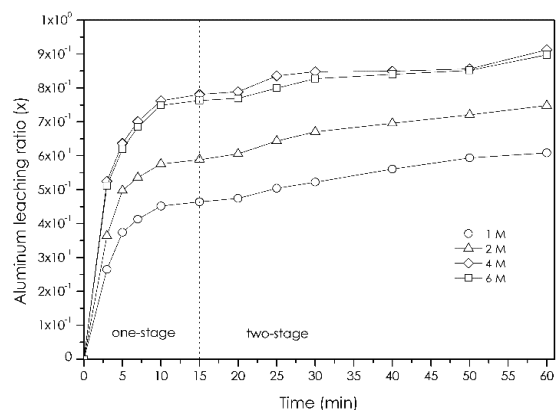


Figure 4 Effect of acid concentration on Al leaching

3.3 Effect of Particle Size

Figure 5 shows that Al leaching ratio increased as particle size decrease from +70-120 mesh to +200-325 mesh. The smaller the particle size, the faster the dissolution [26]. The smaller the particle size can make a large contact surface area thereby increasing Al leaching ratio. The particle size of +200-325 mesh was used for subsequent experiments on effect of temperature.

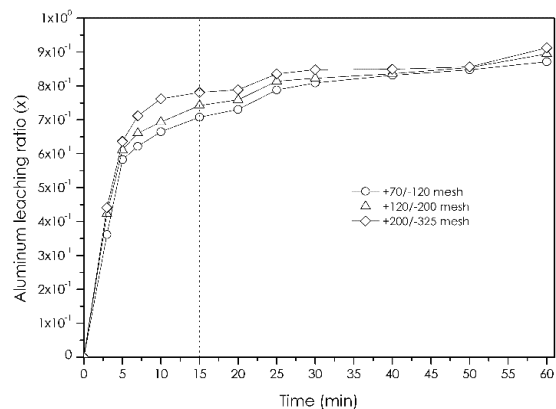


Figure 5 Effect of three different particle sizes on Al leaching

3.4 Effect of Temperature

Figure 6 shows that Al leaching ratio increased with time and temperature. About 91.30% of Al was achieved at HCl of 4 M, 60 min, the particle size of +200-325 mesh with solid/liquid of 0.02 g·ml⁻¹, and temperature of 90 °C. Al leaching was more sensitive to boil temperature above 90 °C, which showed that the diffusion process could be a step not limiting because the layer can be gradually formed on the surface of the particles and not hinder acid from attaining the reactive area at 90 °C and above. This statement contradicts with Cui, *et al.* [25] that Al₂O₃

dissolution from coal mining waste was less sensitive to a temperature between 90 °C and 106 °C, and diffusion process is possible as the rate controlling. However, other researchers describe that the leaching rate will be increased following the increase in temperature [8, 10, 21, 26].

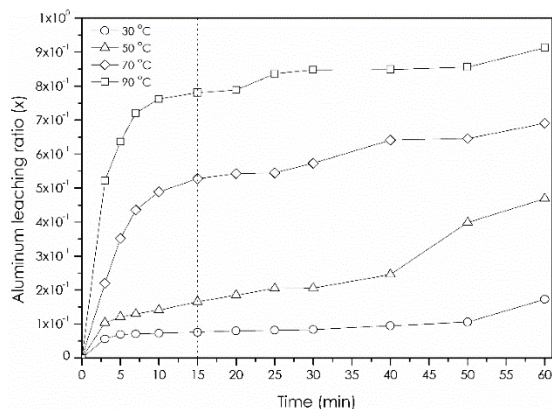


Figure 6 Effect of four different temperatures (at 30-90 °C, 4 M HCl, and particle size of +200-325 mesh)

3.5 Leaching Kinetics

3.5.1 Effect of Acid Concentration

Based on equation (3) and (4) for one-stage and equation (5) and (6) for two-stage the rate constants

Table 5 Values of K_i , K_c and correlation coefficient (R^2) for Al leaching ratio at different acid concentrations (1–6 M)

Acid concentration (M)	One-stage of leaching				Two-stage of leaching			
	Rate constants (min^{-1})		Correlation coefficient (R^2)		Rate constants (min^{-1})		Correlation coefficient (R^2)	
	K_i	K_c	K_i	K_c	K_i	K_c	K_i	K_c
1	0.0090	0.0179	0.9676	0.8808	0.0084	0.0024	0.9862	0.9843
2	0.0160	0.0244	0.9501	0.8595	0.0140	0.0033	0.9752	0.9747
4	0.0325	0.0366	0.9805	0.8834	0.0196	0.0049	0.8582	0.8518
6	0.0309	0.0355	0.9838	0.8865	0.0216	0.0051	0.9521	0.9500

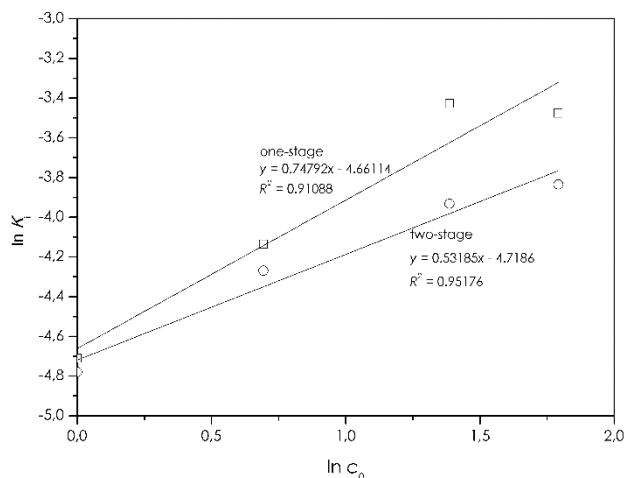


Figure 7 Plots of $\ln K_i$ versus $\ln c_0$ giving the slope as reaction order which c_0 is HCl concentration

determined at dissimilar concentrations are given in Table 5. At the one-stage ($t < 20$ min) and the two-stage of leaching ($t > 20$ min), the correlation coefficient value (R^2) of the rate constant of product layer diffusion (K_i) is higher than the value of the rate constant of surface chemical reaction (K_c). This results indicate that Al leaching ratio is dominated by a product-layer diffusion.

Based on K_i , the logarithm of Al leaching rate constant is illustrated versus the logarithm of acid concentration. The slope in Figure 7 shows the order reaction. It indicate that the Al leaching is both pseudo first order reaction at one-stage and two-stage. The reaction order describes the correlation between acid concentration and aluminum leaching rate. The alteration of HCl concentration was influenced by a higher order reaction [28]. According to Figure 7, Compared to the Al leaching rate for one-stage, the Al leaching rate for two-stage is more influence by HCl concentration. The slope shows that the reaction order is 0.7497 and 0.5318 with a correlation coefficient of 0.9406 and 0.9678 for one-stage and two-stage, respectively. Therefore, the reaction order associated with H^+ ion is near 1 for acid concentrations ≤ 4 M. A similar experiment has been reported by Baba, *et al.* [29] for an order of reaction determination of zinc from spent zinc carbon batteries using HCl.

3.5.2 Effect of Particle Size

The rate constants calculated at three different particle sizes are given in Table 6. The R^2 value of K_i is higher than the value of K_c , implying that Al leaching is controlled by product layer diffusion at one-stage. Similar with the previous section, at two-stage, the R^2 value of K_i is lower than the value of K_c . It means that Al leaching is dominated by surface chemical reaction.

3.5.3 Effect of Temperature

The rate constants calculated at four different temperatures are presented in Table 7. The R^2 value of K_i is higher than the R^2 value of K_c at one-stage. It indicates that the product layer diffusion is controlling leaching process. At two-stage leaching, the

chemical reaction through the surface of the core becomes the rate determining of Al leaching.

In reality, the R^2 value of K_i and an R^2 value of K_c in one-stage and two-stage leaching is different, proposing the probability of two dissimilar reactions take place in the time of leaching continues. This is possibly due to the presence of the other compounds besides Al compound in the peat clay particles. To ensure this hypothesis, the value of activation energy will be calculated by Arrhenius equation. Consequently, in this study, the K value of Arrhenius formula represents the K_i and K_c values for both stage.

The activation energy will be calculated by Arrhenius equation as follows:

$$K = Ae^{-E_a/RT} \quad (7)$$

In a linear shape is

$$\ln K = \ln A - \frac{E_a}{RT} \quad (8)$$

where K is the rate constant, A is the pre-exponential factor, E_a ($\text{kJ}\cdot\text{mol}^{-1}$) is the activation energy, R is the universal gas constant, $8.314 \times 10^{-3} \text{ kJ}\cdot\text{mol}^{-1}\cdot\text{K}^{-1}$, and T is the temperature (K).

Table 6 Values of K_i , K_c and correlation coefficient (R^2) for Al leaching ratio at four different particle size (+70-120; +120-200; and +200-325 mesh)

Particle size (mesh)	One-stage of leaching				Two-stage of leaching			
	Rate constants (min^{-1})		Correlation coefficient (R^2)		Rate constants (min^{-1})		Correlation coefficient (R^2)	
	K_i	K_c	K_i	K_c	K_i	K_c	K_i	K_c
+70-120	0.0239	0.0311	0.9297	0.8840	0.0218	0.0051	0.8862	0.9279
+120-200	0.0265	0.0327	0.9330	0.8699	0.0209	0.0052	0.8971	0.9333
+200-325	0.0343	0.0284	0.9680	0.9171	0.0196	0.0049	0.8518	0.8582

Table 7 Values of K_i , K_c and correlation coefficient (R^2) for Al leaching ratio at different temperature (30, 50, 70, and 90 °C)

Temperature (°C)	One-stage of leaching				Two-stage of leaching			
	Rate constants (min^{-1})		Correlation coefficient (R^2)		Rate constants (min^{-1})		Correlation coefficient (R^2)	
	K_i	K_c	K_i	K_c	K_i	K_c	K_i	K_c
30	0.0002	0.0023	0.8006	0.7005	0.0006	0.0007	0.6940	0.7541
50	0.0007	0.0046	0.9096	0.7663	0.0064	0.0031	0.8701	0.9034
70	0.0112	0.0205	0.9744	0.9554	0.0119	0.0030	0.9604	0.9607
90	0.0333	0.0372	0.9702	0.8817	0.0188	0.0049	0.7361	0.8554

As indicated in Figure 8, the activation energy for both stage was calculated to be $82.79 \text{ kJ}\cdot\text{mol}^{-1}$ and $27.08 \text{ kJ}\cdot\text{mol}^{-1}$. In the present study, the results are not aligned with those given by Brantley, *et al.* [28]; Cui, *et al.* [25]. The activation energy compared with that described by Aarabi-Karagani, *et al.* [24] a lower activation energy ($24\sim 30.12 \text{ kJ}\cdot\text{mol}^{-1}$) means that the leaching kinetics was influenced by a surface reaction, whereas a higher activation energy ($39\sim 90 \text{ kJ}\cdot\text{mol}^{-1}$) shows it is controlled by product layer diffusion [10,30]. Based on this situation, the Al leaching at one-stage is controlled by product layer diffusion while at two-stage, the Al leaching is controlled by surface chemical reaction.

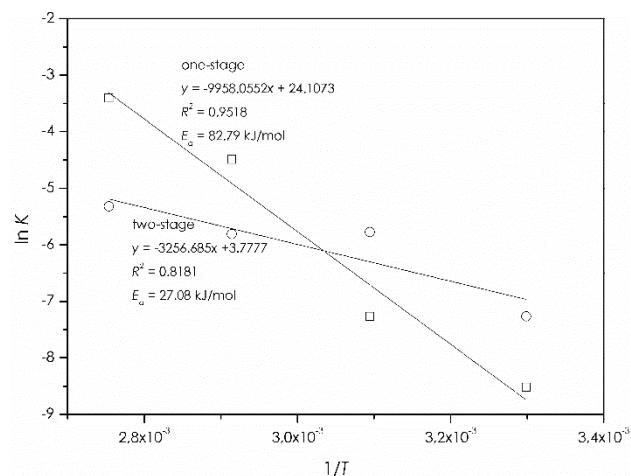


Figure 8 The Arrhenius plot of $\ln K$ against T^{-1} for Al leaching at one-stage and two-stage

4.0 CONCLUSION

The aluminum leaching kinetics from peat clay was performed with four different hydrochloric acid concentration, three different particle size, and four different temperature. The conclusions can be made as follows: Aluminum leaching process was effected by acid concentrations 1 M to 6 M, particle sizes +70-120 mesh to +200-325 mesh, and temperatures 30 °C to 90 °C. From the experiment, about 91.30% of Al was achieved within 60 min at 4 M HCl and 90 °C, using a particle size of +200-325 mesh with solid/liquid of 0.02 g·ml⁻¹ and stirring speed of 300 rpm. The activation energy at one-stage and two-stage was calculated to be 82.79 kJ·mol⁻¹ and 27.08 kJ·mol⁻¹, respectively. The product layer diffusion is controlling the Al leaching at one-stage. However, at two-stage, the Al leaching is controlled by the surface chemical reaction.

Acknowledgement

This experimental study was financially supported by the Directorate General of Higher Education, Ministry of Education and Culture Republic of Indonesia (No. 23428/A4.2/2014) through one of the authors (Agus Mirwan) has been obtained a scholarship for the doctor program from Chemical Engineering Study Program, Lambung Mangkurat University.

References

- [1] Krüger, J. P., Leifeld, J., Glatzel, S., Szidat, S., and Alewell, C. 2015. Biogeochemical Indicators of Peatland Degradation – a Case Study of a Temperate Bog in Northern Germany. *Biogeosciences*. 12(10): 2861-2871.
- [2] Karjalainen, S. M., Ronkanen, A.-K., Heikkinen, K., and Kløve, B. 2016. Long-Term Accumulation and Retention of Al, Fe and P in Peat Soils of Northern Treatment Wetlands. *Ecol. Eng.* 93: 91-103.
- [3] Wendt, H., D. J. O'Connor. 1989. *Alumina Extraction from Non Bauxitic Materials*, Aluminium-Verlag GmbH, Düsseldorf. 1988. 370 Seiten, Preis: DM 160, Berichte Bunsenges. Für Phys. Chem. 93(5): 639-639.
- [4] Ferrier, R. J., Cai, L., Lin, Q., Gorman, G. J., and Neethling, S. J. 2016. Models for Apparent Reaction Kinetics in Heap Leaching: A New Semi-Empirical Approach and Its Comparison to Shrinking Core and Other Particle-Scale Models. *Hydrometallurgy*. 166: 22-33.
- [5] Froment, G. F., and Bischoff, K. B. 1979. *Chemical Reactor Analysis and Design*. Wiley.
- [6] Al-Zahrani, A. A., and Abdel-Majid, M. H. 2004. Production of Liquid Alum Coagulant from Local Saudi Clays. *JKAU Eng Sci.* 15(1): 3-17.
- [7] Al-Ajeel, A. W. A., and Al-Sindy, S. I. A. 2012. Alumina Recovery from Iraqi Kaolinitic Clay by Hydrochloric Acid Route. *Iraqi Bull. Geol. Min.* 2(1): 67-76.
- [8] Al-Zahrani, A. A., and Abdel-Majid, M. H. 2009. Extraction of Alumina from Local Clays by Hydrochloric Acid Process. *JKAU Eng Sci.* 20(2): 29-41.
- [9] Sarkar, S. 2011. The Removal of Alumina and Silica from Iron Rejects Slime by Chemical Leaching. *Hydrometallurgy*. 105(3-4): 364-369.
- [10] Ajemba, R. O., and Onukwuli, O. D. 2012. Application of The Shrinking Core Model to the Analysis of Alumina Leaching From Ukpör Clay Using Nitric Acid. *Int. J. Eng. Res. Technol. IJERT*. 1(3): 1-13.
- [11] Numluk, P., and Chaisena, A. 2012. Sulfuric Acid and Ammonium Sulfate Leaching of Alumina from Lampang Clay. *J. Chem.* 9(3): 1364-1372.
- [12] Ibrahim, A., Ibrahim, I., and Kandil, A. 2013. Preparation of Polyaluminum Chlorides Containing Nano-Al13 from Egyptian Kaolin and Application in Water Treatment. *Tech. J. Eng. Appl. Sci.* 3(13).
- [13] Lima, P. E. A., Angélica, R. S., and Neves, R. F. 2014. Dissolution Kinetics of Metakaolin in Sulfuric Acid: Comparison between Heterogeneous and Homogeneous Reaction Methods. *Appl. Clay Sci.* 88-89: 159-162.
- [14] He, Z., Zhang, Z., Yu, J., Zhou, F., Xu, Y., Xu, Z., Chen, Z., and Chi, R. 2016. Kinetics of Column Leaching of Rare Earth and Aluminum from Weathered Crust Elution-Deposited Rare Earth Ore with Ammonium Salt Solutions. *Hydrometallurgy*. 163: 33-39.
- [15] Altioikka, M. R., and Hoşgün, H. L. 2003. Investigation of the Dissolution Kinetics of Kaolin in HCl Solution. *Hydrometallurgy*. 68(1-3): 77-81.
- [16] Ajemba, R. O., and Onukwuli, O. D. 2012. Kinetic Model for Ukpör Clay Dissolution in Hydrochloric Acid Solution. *J. Emerg. Trends Eng. Appl. Sci. JETEAS*. 3(3): 448-454.
- [17] Melchiori, T., and Canu, P. 2014. Improving the Quantitative Description of Reacting Porous Solids: Critical Analysis of the Shrinking Core Model by Comparison to the Generalized Grain Model. *Ind. Eng. Chem. Res.* 53(22): 8980-8995.
- [18] Nazemi, M. K., Rashchi, F., and Mostoufi, N. 2011. A New Approach for Identifying the Rate Controlling Step Applied to the Leaching of Nickel from Spent Catalyst. *Int. J. Miner. Process.* 100(1-2): 21-26.
- [19] Mirwan, A., Susianto, S., Altway, A., and Handogo, R. 2017. A Modified Shrinking Core Model for Leaching of Aluminum from Sludge Solid Waste of Drinking Water Treatment. *Int. J. Technol.* 8(1): 19.
- [20] Levenspiel, O. 1972. *Chemical Reaction Engineering*. 2nd Edition. New York: Wiley.
- [21] Liddell, Kn. C. 2005. Shrinking Core Models in Hydrometallurgy: What Students Are Not Being Told about the Pseudo-Steady Approximation. *Hydrometallurgy*. 79(1-2): 62-68.
- [22] Jonglertjanya, W., Rattanaphan, S., and Tipsak, P. 2014. Kinetics of the Dissolution of Ilmenite in Oxalic and Sulfuric Acid Solutions. *Asia-Pac. J. Chem. Eng.* 9(1): 24-30.
- [23] Raza, N., Zafar, Z. I., Najam-ul-Haq, and Kumar, R. V. 2015. Leaching of Natural Magnesite Ore in Succinic Acid Solutions. *Int. J. Miner. Process.* 139: 25-30.
- [24] Aarabi-Karagani, M., Rashchi, F., Mostoufi, N., and Vahidi, E. 2010. Leaching of Vanadium from LD Converter Slag Using Sulfuric Acid. *Hydrometallurgy*. 102(1-4): 14-21.
- [25] Cui, L., Guo, Y., Wang, X., Du, Z., and Cheng, F. 2015. Dissolution Kinetics of Aluminum and Iron from Coal Mining Waste by Hydrochloric Acid. *Chin. J. Chem. Eng.* 23(3): 590-596.
- [26] Baba, A. A., and Adekola, F. A. 2012. A Study of Dissolution Kinetics of a Nigerian Galena Ore in Hydrochloric Acid. *J. Saudi Chem. Soc.* 16(4): 377-386.
- [27] Cheng, W.-P., Fu, C.-H., Chen, P.-H., and Yu, R.-F. 2012. Dynamics of Aluminum Leaching from Water Purification Sludge. *J. Hazard. Mater.* 217-218: 149-155.
- [28] Brantley, S. L., Kubicki, J. D., and White, A. F. 2008. *Kinetics of Water-Rock Interaction*. New York: Springer-Verlag.
- [29] Baba, A. A., Adekola, A. F., and Bale, R. B. 2009. Development of a Combined Pyro- and Hydro-Metallurgical Route to Treat Spent Zinc-carbon Batteries. *J. Hazard. Mater.* 171(1-3): 838-844.
- [30] Xue, B., Shao-hua, Y., Yao, L., and Wen-yuan, W. 2011. Leaching Kinetics of Bastnaesite Concentrate in HCl Solution. *Trans Nonferrous Met Soc China*. 21: 2306-2310.